Instrument Science Report COS 2019-04(v1)

The Flux Calibration of the New COS/FUV Cenwave G140L/800

William J. Fischer[1], Ravi Sankrit[1], and Camellia R. Magness[1]

[1] Space Telescope Science Institute, Baltimore, MD

10 May 2019

ABSTRACT

We describe the flux calibration of the new COS/FUV central wavelength (cenwave) setting G140L/800, which uses only segment A of the detector to record wavelengths from 800 to 1950 Å at low resolution. We derived a sensitivity curve by comparing the observed net counts of the spectrophotometric standard WD 0308−565 to a model of the star, and we used this curve to generate an updated FLUXTAB reference file with a flux calibration from 912 to 1950 Å. Counts detected below 912 Å are not currently converted to accurate fluxes by the standard calibration. The reference file was delivered to the database in 2018 November for use by the CalCOS pipeline. Since relatively few cenwave 800 spectra are yet available, limited testing of the flux calibration accuracy has been possible. With the target used to derive the calibration, we find that it is accurate to 2.32%, within the 5% absolute flux accuracy goal of COS. G140L spectra of the supergiant AV 75 obtained with cenwave 800 agree well with those obtained 11 days earlier using G140L cenwaves 1105 and 1280.

Contents

Operated by the Association of Universities for Research in Astronomy, Inc., for the National Aeronautics and Space Administration.

1. Introduction

In Fall 2018 (Cycle 26), two new central wavelength settings (cenwaves G140L/800 and G160M/1533) were introduced for the far-ultraviolet (FUV) channel of the Cosmic Origins Spectrograph (COS). McCandliss et al. (2010) discussed the plausibility of COS observations below 1000 Å, and cenwave 800, intended to maximize the achievable signal-to-noise (S/N) at these wavelengths at low resolution, was first explored in the Cycle 19 general-observer calibration program 12501 (PI S. McCandliss). The mode enables background-limited spectroscopy with the G140L low-resolution grating (resolving power $\sim$ 1000) at wavelengths below 1100 Å. It places wavelengths from 800 to 1950 Å on segment A of the FUV detector, $\sim$ 300 Å below the range of the G140L/1105 cenwave. It does not use segment B, so it avoids the gap between detector segments that affects the G140L/1280 cenwave.

The grating focus for cenwave 800 is chosen to minimize the astigmatic height of the spectrum and therefore the detector background below 1100 Å, allowing higher S/N to be reached for background-dominated targets at these wavelengths than possible with G140L/1280. Redwine et al. (2016) presented a preliminary characterization of this mode and discussed potential science applications, e.g., measurement of Lyman continuum escape fractions at low redshift, exploration of the He II Ly α forest, and determination of abundances in evolved planetary systems of white dwarfs.

Here we discuss the flux calibration of cenwave 800. While a flux calibration was an outcome of the Cycle 19 program, this took place when the COS FUV detector was operating at lifetime position 1 (LP1). Every few years, the lifetime position is changed due to a gradual reduction in the ability of the detector to convert incoming photons to electrons at the current lifetime position. These changes require new calibration efforts; the detector has been operating at LP4 since October 2, 2017. We use the procedure outlined by Debes et al. (2016) for existing cenwaves at LP3 and used by Fischer et al. (2018) for LP4, which is based on the procedure introduced by Massa et al. (2014) for LP1 and LP2 but with less input required from the user. Companion ISRs for cenwave 800 discuss the focus sweep (Sankrit et al. 2019a), the generation of the lamp template (Magness et al. 2019), the spectral extraction (Sankrit et al. 2019b), and the wavelength calibration (Fischer et al. 2019). A similar suite of ISRs is being published for cenwave 1533 by A. Fox, E. Frazer, B. James, and collaborators.

Table 1. Summary of Special Commanding to Configure G140L/800 in APT

Parameter	Value	Description
SPEC COM INSTR	ELOSMTEST	Special commanding instruction
QESIPARM ACTION	TEST	Mode definition
QESIPARM GRATING	G140L	Mode definition
QESIPARM CENTWAVE	800	Mode definition
QESIPARM STEP1	1615	OSM rotation position
QESIPARM RES1	35178	Coarse resolver position
QESIPARM RES2	39803	Fine resolver position
QESIPARM FOCUS4	–1487	Focus position

2. Observations

We obtained G140L/800 data of the spectrophotometric standard WD 0308−565 in Program 15483, "COS FUV G140L/800 Flux Calibration and Cross-Dispersion Profile" (PI R. Sankrit). This target is frequently used for COS flux calibration in various wavelength settings, and high-quality model spectra exist. The star was observed on 2018 June 24. We performed a near-ultraviolet imaging acquisition with a 45 s exposure through the Bright Object Aperture (BOA) with Mirror A in place. For the spectroscopy, we turned off segment B of the FUV detector and observed the target through the Primary Science Aperture (PSA).

The spectroscopy required special commanding because the new cenwave was not implemented in the Astronomer's Proposal Tool (APT) planning software at the time of execution. After the acquisition, we redefined the TEST row to the G140L/800 Optics Select Mechanism (OSM) rotation position (STEP1 = 1615), coarse resolver position (RES1 = 35178), and fine resolver position (RES2 = 39803) determined from ray-trace model predictions (S. Penton, priv. comm.). We set the absolute focus position (FOCUS4 = –1487) as determined from the cenwave 800 focus sweep (Sankrit et al. 2019a). We used the set of APT special-commanding parameters given in Table 1 to make these changes.

Once the TEST row was configured, SQL commanding was required to set QELOGSHEET.MINWAVE to 800 to call the TEST row during each science exposure. At the end of the visit, we restored the TEST row to its default settings using the TEST ACTION RESTORE command. We used special commanding to switch off calibration and disassociate the cenwave 800 exposures, since the back-end software was (at the time of execution) not ready for processing cenwave 800 files.

The general flux calibration requirement for COS spectroscopy is 2% relative accuracy, requiring S/N of 50. Due to the low throughput below 1100 Å, sources bright

enough to reach this S/N threshold in reasonable exposure times would damage the detector at wavelengths longer than 1100 Å. The motivating science case for this mode requires $\sim 10\%$ accuracy (S. McCandliss, priv. comm.), and we chose this as our goal below 1100 Å. Conservatively, we aimed for S/N of 20 in this region and concluded that this could be obtained by binning a spectrum with S/N = 5 per resel by 100 pixels. This requires 1450 s of exposure time, which easily meets the S/N requirement above 1100 Å. We obtained this by using all four FP-POS for 362.5 s per position.

3. Data Reduction

The WD 0308−565 raw data (`rawtag`) files were processed through CalCOS (v3.3.4) with a TWOZONE reduction using newly derived reference files for the LAMPTAB (Magness et al. 2019); DISPTAB and SPWCSTAB (Fischer et al. 2019); and XTRACTAB, TWOZXTAB, PROFTAB, and TRACETAB (Sankrit et al. 2019b). For the FLATFILE, we used a flat field that contains only signatures of gridwires and impostors (Ely et al. 2011), because the routine used to derive the sensitivity curve (Section 4) assumes that no additional components of the flat have been removed from the input spectra. For the FLUXTAB, a file must be provided so that CalCOS creates `x1d` files for use by the flux calibration routine. The actual sensitivity curve in the file is irrelevant, however, because the routine works on the counts in the `x1d` files, not the fluxes. We used a preliminary version based on the Cycle 19 calibration program.

All calibration switches were set to their default values, except the time-dependent sensitivity switch TDSCORR was set to OMIT, since there was no information yet on the time dependence of the sensitivity of the new cenwaves.

4. Deriving the Flux Calibration

We followed the procedure used to calibrate the existing cenwaves at LP3 and LP4, described by Debes et al. (2016) and Fischer et al. (2018), respectively, which is based on the IDL procedure `derive_cos_flats.pro` by G. Becker. This method assumes that the net counts in each `x1d` file are the product of the flux from the source, the flat field, and the sensitivity, or

$$N(x, \lambda) = S(\lambda)F(x)R(\lambda),$$

where $N(x, \lambda)$ are the net counts at detector position x (XFULL) and wavelength λ, $S(\lambda)$ is the flux, $F(x)$ is the flat field, and $R(\lambda)$ is the response (sensitivity) function. The goal of the flux calibration is to derive $R(\lambda)$ for cenwave 800 and use it to generate a FLUXTAB reference file.

The standard approach to the calibration of COS data assumes that the flat field depends on detector position and grating but not on cenwave. For cenwave 800, we thus adopted the flat field already in place for G140L at LP4 (`19m1548jl_flat.fits`,

derived by Fischer et al. 2018) instead of deriving a new one. This is accomplished in the flux calibration routine by setting the keyword `fixed_flat` equal to the name of a FITS file that contains the existing flat field as a 1D array.

We used the latest model spectrum of WD 0308−565 from Bohlin et al. (2014; file `wd0308_565_mod_003.fits`) and convolved it with a line-spread function derived for cenwave 800 at LP4 by E. Elliot[1]. We then divided the counts in the `x1d` file at each FP-POS position by the flat and the model, masking Ly α and other lines. All remaining variations of low spatial frequency are then expected to be due to varying sensitivity, and the result from each FP-POS is treated as an independent measurement of the sensitivity. We binned the results by 50 pixels and performed piecewise quadratic interpolation to generate the final curve. There were 38 knots for the interpolation, ranging from 911 Å to 1165 Å at 13 Å spacing and from 1165 Å to 1943 Å at 43 Å spacing. This scheme accommodates the more rapidly fluctuating wavelength dependence of the sensitivity below 1165 Å.

With the Python procedure `make_fluxtab.py`, we added new rows to the LP4 FLUXTAB for the PSA and the BOA. The PSA sensitivity is the curve calculated above, interpolated to 2730 wavelengths ranging from 911 Å to 1943 Å, in units of counts per unit flux density; i.e., counts (erg s^{-1} cm^{-2} $Å^{-1}$)$^{-1}$. It is shown in Figure 1; broadly, it is seen to be consistent with the sensitivities of the other G140L modes at LP4 (Fischer et al. 2018). The BOA sensitivity is simply the PSA sensitivity times the BOA transmission (Massa et al. 2010).

Cenwave 800 allows counts to be recorded below 912 Å to wavelengths as short as 800 Å. The sensitivity over these shortest wavelengths is currently set to an artificially large value, such that counts at these wavelengths are converted to artificially small fluxes, not intended for immediate science use but still available for observers to apply their own calibrations. This is consistent with the handling of such wavelengths with the existing G140L/1280 cenwave, which places this range on segment B of the detector.

5. Testing the Flux Calibration

We recalibrated the WD 0308−565 dataset with the CalCOS pipeline using the new FLUXTAB and the appropriate FLATFILE, which was derived for G140L spectroscopy at LP4 using data from the existing cenwaves 1105 and 1280. All other calibration switches and reference files were identical to those given in Section 3. This yielded flux-calibrated spectra for testing.

We first tested the resulting flux calibration of the cenwave 800 data by comparing the calibrated spectrum of WD 0308−565 to its model. The result of this test appears in Figure 2. The top panel plots the observed spectrum, binned by 60 pixels, over the model. The bottom panel shows the fractional difference, i.e., the data minus the model, divided by the model. Regions containing the lines visible in the model and the edges

[1] `http://www.stsci.edu/hst/cos/performance/spectral_resolution/`

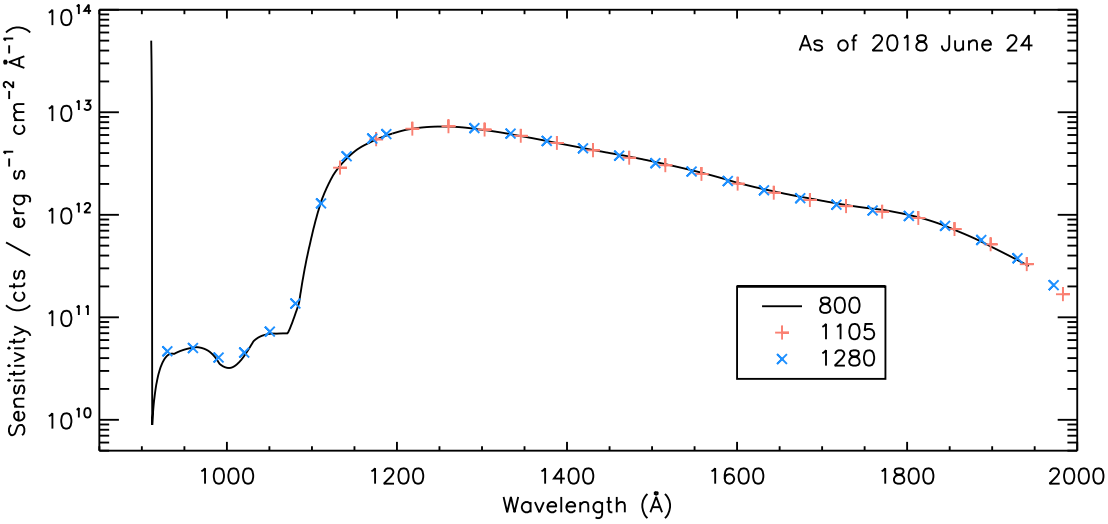

Figure 1. The G140L/800 sensitivity curve derived from spectra of WD0308−565. Note the y-axis is logarithmic. The large value at the shortest wavelength allows counts below 912 Å to remain in the final spectrum at artificially small fluxes pending a reliable calibration there. For comparison, the sensitivity curves for the other G140L modes, corrected to the time of the G140L/800 observations, are also shown at select wavelengths. They agree well with the result for cenwave 800.

of the detector, including the entire region below 912 Å, are excluded from the bottom plot. The mean difference between the data and the model is −0.135%, and the standard deviation is 2.32%.

Figure 3 shows another test of the flux calibration. Cenwave 800 spectra of the O5 supergiant AV 75 were obtained in our focus sweep program 15451 (PI W. Fischer; see Sankrit et al. 2019a). Fourteen spectra were obtained at different grating focus positions; here we analyze the one with the focus value that was ultimately adopted. Spectra of the same star were obtained 11 days earlier in program 15385, "COS FUV Wavelength Scale Monitor" (PI W. Fischer) with the existing G140L cenwaves, 1105 and 1280. The cenwave 800 spectrum was calibrated with the sensitivity curve discussed here and incorporated in the new FLUXTAB, while the other spectra were calibrated with the sensitivity curves already derived for LP4 by Fischer et al. (2018).

In the top panel of the figure, we plot all three spectra, binned by ten pixels. The cenwave 1105 and 1280 spectra each had 80 s of exposure time at a single FP-POS; their reduced S/N is apparent compared to the cenwave 800 spectrum, which had four FP-POS at a total of 1450 s. Nonetheless, the spectra overlap quite well. The bottom panel of the figure shows the ratio of the fractional difference, i.e., cenwave 1105 or 1280 minus cenwave 800, divided by cenwave 800. Here the spectra are binned by 60 pixels, as in Figure 2. The edges of the detector, including the entire region below 912 Å, and the region affected by Ly α airglow are excluded from the bottom plot.

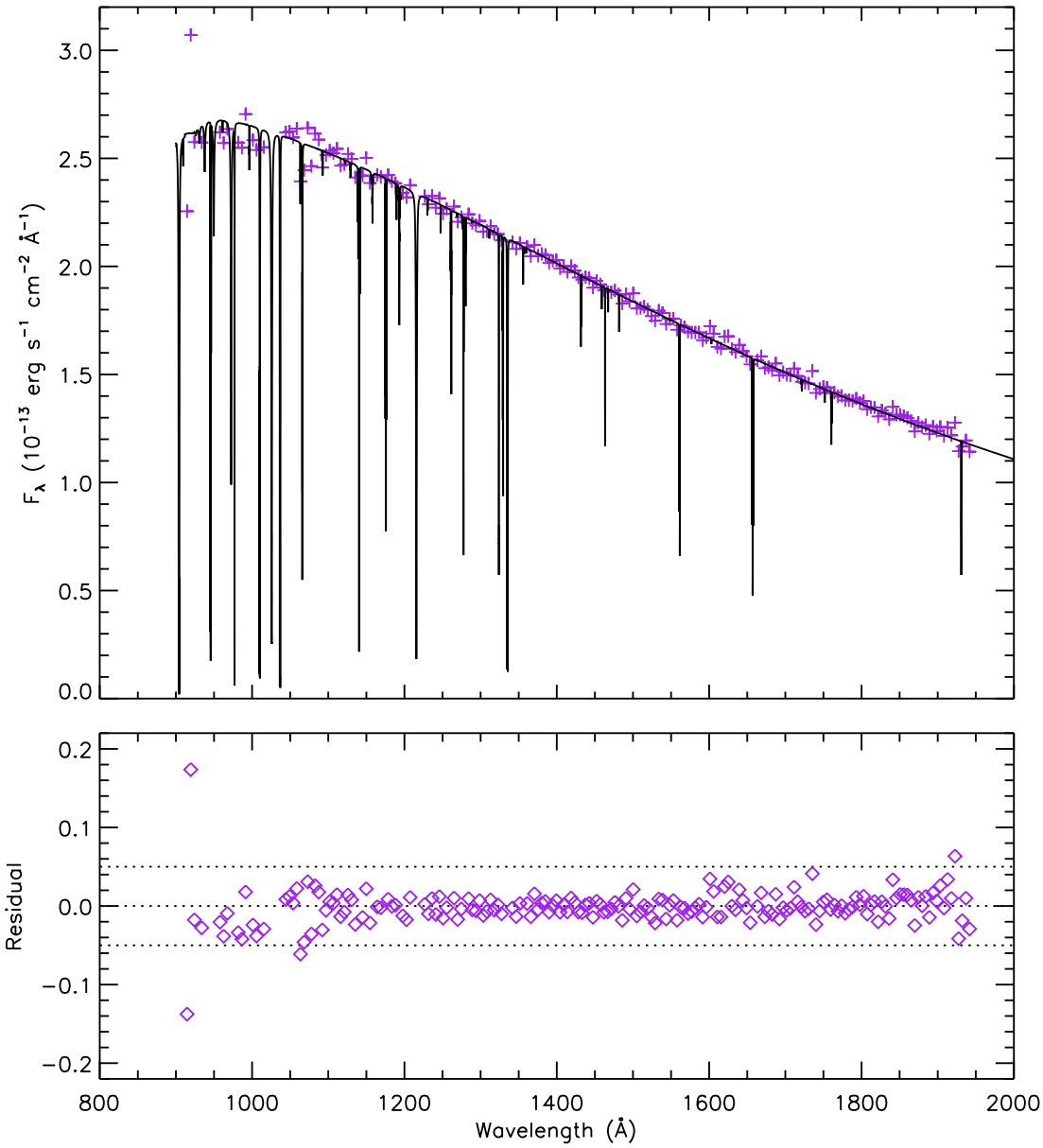

Figure 2. Demonstration of the accuracy and precision of the flux calibration for cenwave 800. *Top:* The cenwave 800 spectrum of WD 0308−565, binned by 60 pixels (purple), and the model spectrum (black). *Bottom:* Residuals, i.e., the data minus the model, divided by the model. Absorption and airglow lines and the detector edges, including the entire region below 912 Å, are excluded from the analysis. Dotted lines at ± 5% serve to guide the eye. Although further testing with additional targets is needed for an independent assessment, the small scatter in the residuals (standard deviation = 2.32%) suggests good flux calibration.

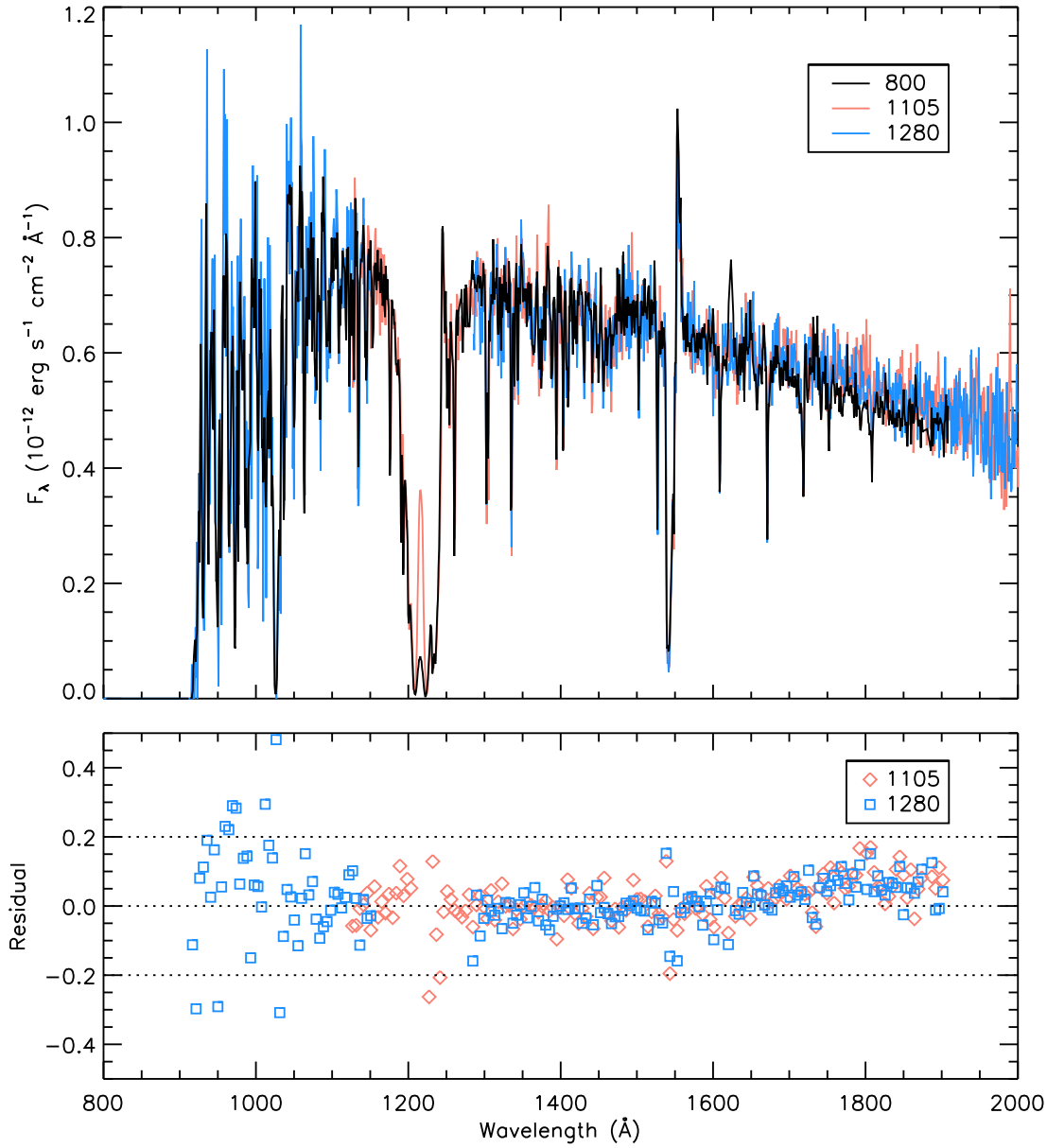

Figure 3. A comparison of a cenwave 800 spectrum of AV 75 to those of the same star obtained 11 days earlier with the other G140L cenwaves, 1105 and 1280. *Top:* The cenwave 800 spectrum (black) and the cenwave 1105 and 1280 spectra (salmon and light blue), plotted with ten-pixel binning. *Bottom:* Residuals, i.e., cenwave 1105 or 1280 minus cenwave 800, divided by cenwave 800. The edges of the detector, including the entire region below 912 Å, and the region affected by Ly α airglow are excluded from the analysis. Dotted lines at $\pm$ 20% serve to guide the eye. The continua agree to within 5% over most of the wavelength range; discrepancies are discussed in the text.

The residuals are large below 1100 Å; the new cenwave is designed to enable an improvement there in S/N compared to cenwave 1280. Residuals are also large near the strongest lines in the AV 75 spectrum, likely due to the intrinsic variability of the star over 11 days. Above 1100 Å, the continua agree to within about 5%, except for a decline of about 10% in the cenwave 800 flux beyond 1650 Å. This discrepancy at long wavelengths is likely due to stellar variability, but it may be investigated in more detail as additional cenwave 800 spectra become available.

6. Summary

The cenwave 800 sensitivity curves for both the PSA and BOA were merged into the FLUXTAB submitted to the CRDS reference-file database on 2018 November 20. The new FLUXTAB (`2bj2256gl_phot.fits`) contains the sensitivity curves for both new cenwaves G160M/1533 and G140L/800 as well as sensitivity curves for all previously existing cenwaves; it is in use for observations at LP4 in Cycle 26 and beyond. Comparing the observed and model spectra of WD 0308−565, we find a standard deviation of 2.32% across the wavelength range. G140L spectra of AV 75 obtained with cenwave 800 agree well with those obtained 11 days earlier with cenwaves 1105 and 1280. Scripts discussed in this ISR have been placed in the `cos/newcenwave_c800` repository on the internal STScI GitLab site. Interested parties at other institutions may contact the team for more information about them.

Acknowledgments

We thank the rest of the COS new cenwaves team for their support: Andy Fox, Elaine Frazer, Bethan James, Julia Roman-Duval, Gisella de Rosa, and Cristina Oliveira.

Change History for COS ISR 2019-04

Version 1: 10 May 2019 – Original Document

References

Bohlin, R., Gordon, K. D., & Tremblay, P.-E. 2014, PASP, 126, 711

Debes, J. H., Becker, G., Roman-Duval, J., et al. 2016, COS ISR 2016-15, "Third COS FUV Lifetime Calibration Program: Flatfield and Flux Calibrations"

Ely, J., Massa, D., Ake, T., et al. 2011, COS ISR 2011-03, "COS FUV Gridwire Flat Field Template"

Fischer, W. J., Magness, C. R., Sankrit, R., & Oliveira, C. 2019, COS ISR 2019-05, "The Dispersion Solution for the New COS/FUV Cenwave G140L/800"

Fischer, W. J., Rafelski, M., & de Rosa, G. 2018, COS ISR 2018-20, "Flat Fields and Flux Calibrations for the COS FUV Channel at Lifetime Position 4"

Magness, C. R., et al. 2019, COS ISR 2019-02, “Lamp Template for the New COS/FUV Cenwave G140L/800”

Massa, D., Ely, J., Osten, R., et al. 2014, COS ISR 2013-09, “Updated Absolute Flux Calibration of the COS FUV Modes”

Massa, D., Keyes, C., Penton, S., Bohlin, R., & Froning, C. 2010, COS ISR 2010-02, “SMOV Absolute Flux Calibration of the COS FUV Modes”

McCandliss, S. R., France, K., Osterman, S., et al. 2010, ApJL, 709, L183

Redwine, K., McCandliss, S. R., Zheng, W., et al. 2016, PASP, 128, 105006

Sankrit, R., Fischer, W. J., Magness, C. R., & Fox, A. J. 2019a, COS ISR 2019-01, “Focus Sweep for the New COS/FUV Cenwave G140L/800”

Sankrit, R., Magness, C. R., Fischer, W. J., Frazer, E. M., & Roman-Duval, J. 2019b, COS ISR 2019-03, “Spectral Extraction for the New COS/FUV Cenwave G140L/800”